The Journal of Immunology

Impaired Macrophage Function Underscores Susceptibility to *Salmonella* in Mice Lacking Irgm1 (LRG-47)

Stanley C. Henry, Xiaojou Daniell, Maanasa Indaram, John F. Whitesides, Gregory D. Sempowski, David Howell, Tim Oliver and Gregory A. Taylor

J Immunol 2007; 179:6963-6972; ;
doi: 10.4049/jimmunol.179.10.6963
http://www.jimmunol.org/content/179/10/6963

This information is current as of July 19, 2018.

References This article **cites 42 articles**, 24 of which you can access for free at:
http://www.jimmunol.org/content/179/10/6963.full#ref-list-1

Why *The JI*? Submit online.

- **Rapid Reviews! 30 days*** from submission to initial decision
- **No Triage!** Every submission reviewed by practicing scientists
- **Fast Publication!** 4 weeks from acceptance to publication

**average*

Subscription Information about subscribing to *The Journal of Immunology* is online at:
http://jimmunol.org/subscription

Permissions Submit copyright permission requests at:
http://www.aai.org/About/Publications/JI/copyright.html

Email Alerts Receive free email-alerts when new articles cite this article. Sign up at:
http://jimmunol.org/alerts

The Journal of Immunology is published twice each month by
The American Association of Immunologists, Inc.,
1451 Rockville Pike, Suite 650, Rockville, MD 20852
Copyright © 2007 by The American Association of Immunologists All rights reserved.
Print ISSN: 0022-1767 Online ISSN: 1550-6606.

Downloaded from http://www.jimmunol.org/ by guest on July 19, 2018

Impaired Macrophage Function Underscores Susceptibility to *Salmonella* in Mice Lacking Irgm1 (LRG-47)[1]

Stanley C. Henry,* Xiaojou Daniell,[†‡§] Maanasa Indaram,[†‡§] John F. Whitesides,[¶] Gregory D. Sempowski,[¶] David Howell,[#] Tim Oliver,[‖] and Gregory A. Taylor[2]*[†‡§]

IRG proteins, or immunity-related GTPases (also known as p47 GTPases), are a group of IFN-regulated proteins that are highly expressed in response to infection. The proteins localize to intracellular membranes including vacuoles that contain pathogens in infected macrophages and other host cells. Current data indicate that the IRG protein Irgm1 (LRG-47) is critical for resistance to intracellular bacteria. This function is thought to be a consequence of regulating the survival of vacuolar bacteria in host cells. In the current work, the role of Irgm1 in controlling resistance to *Salmonella typhimurium* was explored to further define the mechanism through which the protein regulates host resistance. Irgm1-deficient mice displayed increased susceptibility to this bacterium that was reflected in increased bacterial loads in spleen and liver and decreased maturation of *S. typhimurium* granulomas. The mice also displayed an inability to concentrate macrophages at sites of bacterial deposition. In vitro, the ability of Irgm1-deficient macrophages to suppress intracellular growth of *S. typhimurium* was impaired. Furthermore, adhesion and motility of Irgm1-deficient macrophages after activation with IFN-γ was markedly decreased. Altered adhesion/motility of those cells was accompanied by changes in cell morphology, density of adhesion-associated proteins, and actin staining. Together, these data suggest that in addition to regulating the maturation of pathogen-containing vacuoles, Irgm1 plays a key role in regulating the adhesion and motility of activated macrophages. ***The Journal of Immunology,*** **2007, 179: 6963–6972.**

The cytokine IFN-γ is critical for innate immunity to intracellular pathogens (1–4). IFN-γ regulates immunity, in large part, by stimulating the expression of proteins that serve as effectors of IFN-γ-regulated processes. Among these proteins is a group of mammalian proteins that are known as immunity-related GTPases (IRGs),[3] also known as p47 GTPases (5–9). This family of GTP-binding proteins is essential for IFN-γ-regulated resistance to intracellular bacteria and protozoa, with different GTPases being required for resistance to different groups of pathogens (9). Although progress has been made in defining their roles in host resistance, detailed mechanisms that underlie their functions have not been determined.

To date, p47 GTPase research has focused mainly on seven mouse proteins known as Irgm1 (LRG-47) (10), Irgm2 (GTPI) (11), Irgm3 (IGTP) (12), Irgd (IRG-47) (13), Irga6 (IIGP1) (11), Irgb6 (TGTP) (7, 14, 15), and Irgb10 (16). The overriding roles of the proteins in host defense were initially defined by characterizing the responses of gene-targeted mice that lacked expression of Irgm1, Irgm3, and Irgd to pathogens (17, 18). These and subsequent studies have shown, in general, that Irgm1 is required for resistance to a broad range of intracellular bacteria and protozoa; Irgm3 is required for resistance to a smaller group of protozoa and a very limited range of bacteria such as *Chlamydia trachomatis* (16); and Irgd plays a more limited role in host resistance (6, 8, 9). The basis for their different roles in host resistance is not yet clear. IRG proteins appear to be expressed at high levels in a variety of hemopoietic and nonhemopoietic cells following parasitic and bacterial infection. Within these cells, they are bound to intracellular membranes to varying degrees, ranging from 90% membrane-bound for Irgm1 and Irgm3 (19, 20) to <10% membrane bound for Irgd (20). The bulk of the membrane-bound forms of the proteins localizes to the endoplasmic reticulum and/or Golgi compartments (19, 20), but importantly, the proteins have also been found at the plasma membrane (20) and in pathogen-containing vacuoles in macrophages and astrocytes (20–22).

Multiple studies now support a role for IRG proteins in suppressing the intracellular survival of protozoa and bacteria in host cells, including macrophages and astrocytes. These data implicate Irgm3 in restricting *Toxoplasma gondii* (22, 23) and *C. trachomatis* (16) survival; Irgm1 in restricting *Mycobacterium tuberculosis* (24), *Trypanosoma cruzi* (25), and *Toxoplasma gondii* (22); Irga6 in restricting *T. gondii* (21); and Irgd in restricting *T. cruzi* (26). Because IRG proteins often localize to pathogen-containing vacuoles as the pathogen enters the host cell and remain with the vacuole as it is processed (20, 22), it has been suggested that the proteins regulate processing of pathogen-containing vacuoles, thereby governing growth and survival of the pathogen. At least three different mechanisms have been suggested through which IRG proteins may regulate survival of vacuolar pathogens, although these mechanisms are not necessarily exclusive. The

*Geriatric Research, Education, and Clinical Center, Veterans Affairs Medical Center, Durham, NC 27705; [†]Department of Medicine, [‡]Department of Molecular Genetics and Microbiology, and [§]Department of Immunology, Division of Geriatrics and Center for the Study of Aging and Human Development, Duke University Medical Center; [¶]Department of Medicine, Human Vaccine Institute; [‖]Department of Cell Biology, Duke University Medical Center, Durham, NC 27710; and [#]Department of Pathology, Duke University and Durham Veterans Affairs Medical Centers, Durham, NC 27705

Received for publication December 22, 2006. Accepted for publication September 6, 2007.

The costs of publication of this article were defrayed in part by the payment of page charges. This article must therefore be hereby marked *advertisement* in accordance with 18 U.S.C. Section 1734 solely to indicate this fact.

[1] This work was funded by National Institutes of Health Grant AI57831.

[2] Address correspondence and reprint requests to Dr. Gregory A. Taylor, Duke University, Box 3003, Duke University Medical Center, Durham, NC 27710. E-mail address: gregory.taylor@duke.edu

[3] Abbreviations used in this paper: IRG, immune-regulated GTPase; BMM, bone marrow macrophage; WT, wild type; LDH, lactate dehydrogenase; PMN, polymorphonuclear cell.

Downloaded from http://www.jimmunol.org/ by guest on July 19, 2018

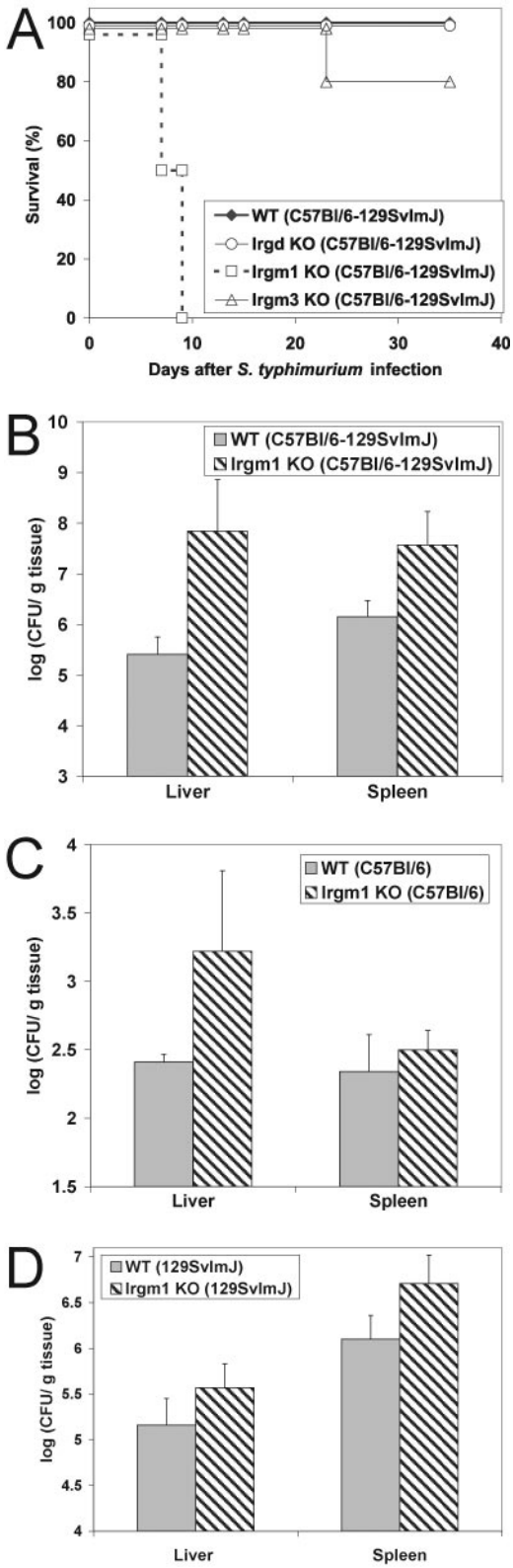

FIGURE 1. Decreased resistance to *S. typhimurium* in Irgm1-deficient mice. *A*, WT ($n = 5$), Irgm1 KO ($n = 4$), Irgm3 ($n = 5$), and Irgd KO mice ($n = 4$) (all on a C57BL/6-129SvIm/J hybrid background) were inoculated i.v. with 10^6 CFU of *S. typhimurium*. Shown is survival of the mice. *B–D*, Groups of at least five mice of the indicated strains were inoculated i.v. with 10^6 CFU of *S. typhimurium*. Six days later, spleen and liver were isolated and used for CFU determination. *B*, The mice were on a C57BL/6-129SvIm/J hybrid background; *C*, a C57BL/6 background; and *D*, a 129SvIm/J background. Error bars, SDs. In each case, the increases in bacterial levels in Irgm1-deficient tissues relative to those in WT tissues were statistically significant; for liver and spleen, respectively, p values were 0.006 and 0.012 in *B*, 0.011 and 0.04 in *C*, and 0.04 and 0.008 in *D*.

earliest to be proposed is that the IRG proteins promote maturation of the pathogen-containing vacuoles, as evidenced by decreased acidification and lysosome fusion of *M. tuberculosis* vacuoles in Irgm1-deficient macrophages (24). Other studies have demonstrated that Irga6 (21) and Irgm3 (27) promote "vesiculation" or breakdown of the *T. gondii* vacuole in astrocytes and macrophages, leading to denuding of the pathogen and loss of intracellular survival. Finally, a third mechanism suggests that the proteins cause pathogen-containing vacuoles to enter an autophagic pathway that leads to the demise of the pathogen, evidence for which comes from experiments studying the roles of mouse Irgm1 (28) and human IRGM (29) in controlling survival of *M. tuberculosis* in macrophages and in studying the role of Irgm3 in controlling *T. gondii* in macrophages (27). It remains to be determined whether IRG proteins possess multiple functions or whether they have a single function with varying manifestations in these different contexts.

In the current article, we further explore the role of Irgm1 in host resistance, using *Salmonella typhimurium* as a model bacterial pathogen and focusing on macrophage-based mechanisms of host resistance. We find not only that Irgm1 regulates survival of *S. typhimurium* in macrophages, a function that has been documented for Irgm1 using other pathogen models as mentioned above, but that Irgm1 has wider reaching effects on macrophage function than previously appreciated, including the regulation of adhesion and motility of the cells following activation by IFN-γ.

Materials and Methods

Mice and cell culture

Irgm1 (LRG-47)-deficient, Irgm3 (IGTP)-deficient, and Irgd (IRG-47)-deficient mice used in these experiments have been described previously (18) and were generated and maintained according to Institutional and Animal Car Committee-approved protocols at the Durham Veterans Affairs and Duke University Medical Centers. The genetic backgrounds of the mice were C57BL/6 × 129 SvImJ hybrid, C57BL/6 (backcrossed for nine generations), or 129 SvImJ (backcrossed for six generations). All three backgrounds were used in the experiments described in Fig. 1, whereas the remaining studies used only mice on the C57BL/6 background.

Primary murine bone marrow macrophages (BMM) were isolated from the tibia and femurs of 2- to 4-mo-old mice. Bone marrow was flushed from the bones using a 27-gauge syringe filled with DMEM (Invitrogen Life Technologies), the marrow was dispersed by drawing through the needle three to four times, and RBC were lysed with ammonium chloride. Adherent cells were cultured in BMM medium (DMEM supplemented with 10% (v/v) FBS; HyClone) and 30% (v/v) L929 cell-conditioned medium) for 5–6 days. The cells were cultured on petri dishes that were not cell culture treated, which resulted in cultures that were loosely adherent and easily removed from the plates with Cell Dissociation Buffer (no. 13150-016; Invitrogen Life Technologies). Twenty-four hours before all experiments, the cells were placed in medium lacking L929-conditioned medium (DMEM supplemented with 10% (v/v) FBS). Both wild-type (WT) and Irgm1-deficient BMM were found to be at least 95% positive for the F4/80 macrophage marker.

Bacteria

Two strains of *S. typhimurium* were used in these studies: a virulent strain SL1344 (30) and an aroA$^-$ strain SL7731 (31, 32). The bacteria were cultured overnight in Luria-Bertani (LB) broth without shaking.

In vivo bacterial infection

Bacteria were injected i.v. at 6×10^5 cells/mouse in a volume of 0.1 ml of PBS. The SL7731 strain was used; it has a strong requirement for IFN-γ-induced mechanisms for host resistance (32) and is more easily handled

Downloaded from http://www.jimmunol.org/ by guest on July 19, 2018

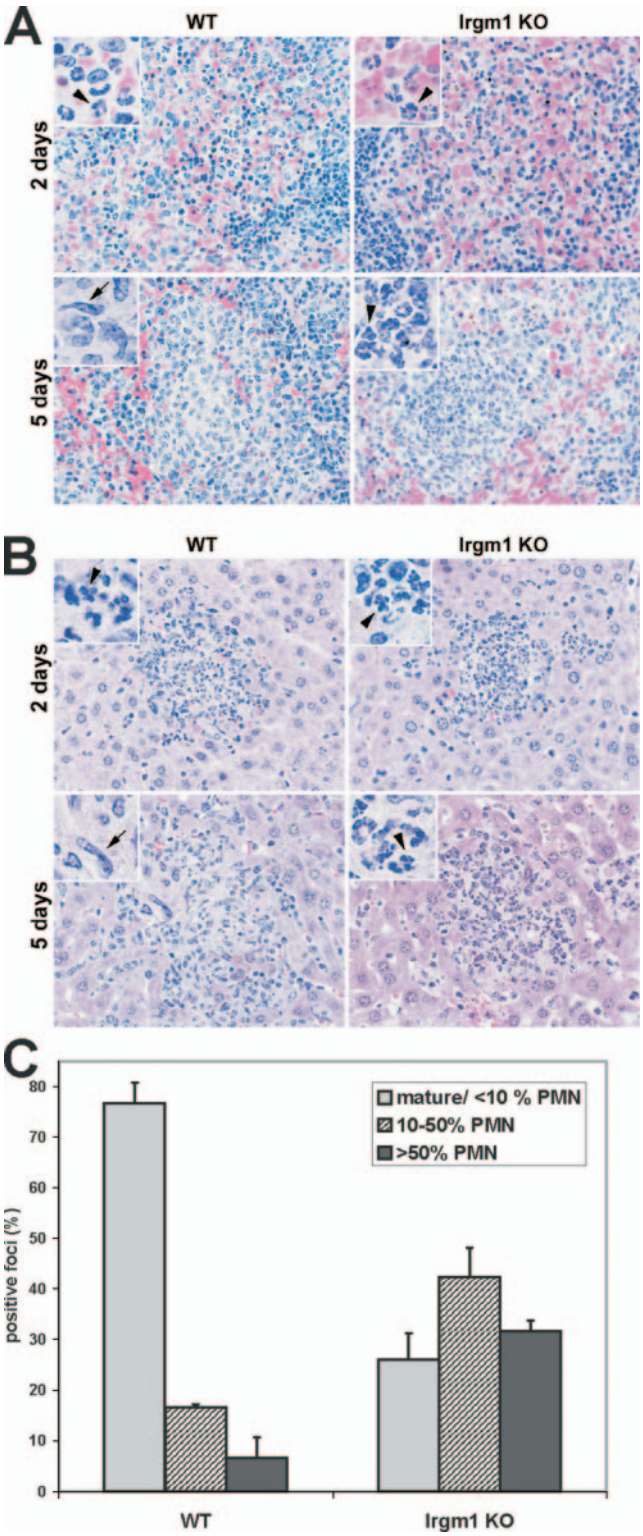

FIGURE 2. Impaired maturation of *S. typhimurium* granulomas in Irgm1-deficient mice. WT (C57BL/6) and Irgm1 KO mice were inoculated i.v. with 10^6 CFU of *S. typhimurium*. At 2 and 5 days after infection, tissues were isolated, fixed, and used for H&E staining. *A* and *B*, Typical lesions are shown from days 2 and 5, in spleen and liver, respectively. Cells from the lesions at a higher magnification are shown in the *insets*. Note that at day 2, the foci from WT and Irgm1-deficient mice were immature, containing predominantly PMNs (arrowheads). By day 5, the majority of foci in the livers of WT mice were well-organized granulomas rich in epithelioid cells (arrows), while those in Irgm1-deficient mice were immature, containing primarily PMNs. *C*, Inflammatory foci were enumerated in a blinded fashion from the livers of three mice per genotype at 5 days postinfection. One hundred foci were counted per sample. Each focus was assigned to one of three classes: category 1, mature granulomas composed of <10% PMNs/>90% epithelioid cells; category 2, less mature foci containing 10–50% PMNs; or category 3, the least mature foci containing >50% PMNs. Differences in the numbers of foci for each category between WT and Irgm1 KO livers were statistically significant ($p = 0.006$, 0.020, and 0.002, for categories 1, 2, and 3, respectively).

than the fully virulent strain. Inoculated mice were either followed for survival or bacterial counts were determined by excising spleens and livers sterilely, homogenizing portions of the organs in PBS, and plating serial dilutions of the homogenate on LB agar plates. Colony counts were assessed the following day, from which the total bacterial load per organ was calculated.

Western blotting

Western blots were performed according to standard protocols using anti-Irgm1 (LRG-47) and anti-Irgm3 (IGTP) Abs as described previously (12, 18).

Histology

Spleen and liver tissues were isolated from mice that had been infected with *S. typhimurium* for the times indicated in the text. Tissues were preserved in buffered formalin and then processed for paraffin sectioning and H&E staining.

Splenocyte phenotyping

The spleens of mice infected with *S. typhimurium* were isolated; spleen cells were disaggregated and filtered through a cell strainer; RBC were lysed with ammonium chloride lysis; and the remaining splenocytes were concentrated by centrifugation at 500 × *g*. Direct immunofluorescence staining was performed with anti-mouse, directly conjugated mAbs: anti-CD3 PE (BD Biosciences), anti-Gr1 allophycocyanin (BD Biosciences), anti-F4/80 PE-Cy5.5 (Caltag Laboratories), and anti-CD68-RPE (Serotec). Surface staining was accomplished by mixing the cells with the diluted Abs in PBS-Wash (PBS plus 1% (w/v) BSA plus 0.1% (w/v) sodium azide), incubating for 45 min at 4°C, and then washing. Internal staining (for CD68) was accomplished by permeabilizing the cells with 0.5% (w/v) saponin in PBS-Wash, incubating with the Ab in PBS-Wash/saponin for 45 min at 4°C, and then washing. Stained cells were fixed with 0.4% paraformaldehyde (w/v). Immunophenotype data were acquired on a FACSVantage SE (BD Biosciences) and data were analyzed with FlowJo software (Tree Star; Duke University Human Vaccine Institute Flow Facility, Durham, NC). T cells were defined as CD3-positive cells, macrophages as $CD68^{high}F4/80^{int\text{-}high}Gr1^{low}$ cells, and neutrophils as $CD68^{low}F4/80^{low}Gr1^{high}$ cells (33).

In vitro bacterial survival assays

BMM were plated in 24-well plates at 0.35×10^6 cells/well. They were exposed to varying concentrations of IFN-γ (EMD Biosciences/Calbiochem) for 24 h. The cells were infected with *S. typhimurium* at a multiplicity of infection of two bacteria per macrophage. The bacteria were added as a suspension in DMEM, the plates were centrifuged at 250 × *g* for 5 min, incubated for an additional 10 min, and washed three times with DMEM to remove extracellular bacteria. The cells were then incubated for various times in medium supplemented with 6 μg/ml gentamicin. To quantify bacterial levels, the cells were washed with DMEM three times and then lysed with 0.2% (v/v) Triton X-100 in PBS. Dilutions of the lysates were plated on LB plates and CFU were counted. The assay was performed in triplicate for each condition.

Adhesion assay

BMM were plated on glass coverslips in 24-well plates at 0.35×10^6 cells/coverslip. The coverslips had been coated with 10 μg/ml human plasma fibronectin in PBS for 2 h or had been left uncoated. Twenty-four hours after plating the cells, they were exposed to 100 U/ml IFN-γ for 24 h. The cells were then washed with PBS without Ca^{2+}/Mg^{2+} four times to remove loosely adherent cells, fixed with 4% (w/v) paraformaldehyde/PBS for 10 min, stained with 0.5% (w/v) crystal violet/methanol for 10 min, and washed five times with water to remove excess stain. Finally, the cells were solubilized in methanol overnight at 4°C, and the absorbance at 595 nm was read as a measure of adherent cells.

Downloaded from http://www.jimmunol.org/ by guest on July 19, 2018

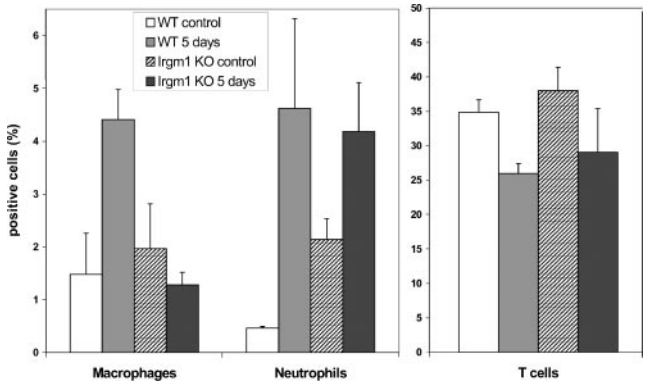

FIGURE 3. Impaired macrophage accumulation in spleens of Irgm1-deficient mice following *S. typhimurium* infection. Groups of three WT and Irgm1-deficient mice were inoculated i.v. with 10^6 CFU of *S. typhimurium* or left uninfected. At 5 days postinfection, splenocytes were isolated and used for flow cytometric analysis. Shown are percent positive cells for the indicated populations. Macrophages were defined as $CD68^{high}F4/80^{int\text{-}high}Gr1^{low}$ cells, neutrophils as $CD68^{low}F4/80^{low}Gr1^{high}$ cells, and T cells as $CD3^+$. Data shown are representative of three studies. Error bars, SDs for this study. The decreased macrophage levels in infected Irgm1 KO mice were statistically significant, relative to levels in infected WT mice ($p = 0.005$).

Transwell motility assay

Standard Transwell devices in a 24-well format (Corning) were used that had an upper chamber separated from a lower chamber by a polycarbonate membrane containing 5-μm pores. The lower surface of the porous membrane was coated with human fibronectin. Twenty-four hours before the experiment, BMM were placed in medium that lacked L929-conditioned medium, but contained in some cases 100 U/ml IFN-γ. These cells were dislodged with Cell Dissociation Buffer, enumerated with a hemocytometer using trypan blue to exclude dead cells, and then placed in the upper chamber of Transwell devices in medium lacking L929-conditioned medium and IFN-γ. (Note that after removing IFN-γ from activated WT BMM, the cells retained high Irgm1 expression for at least 24 h (data not shown).) In the lower chamber of the Transwell device, BMM medium (containing L929-conditioned medium, a source of the chemoattractant M-CSF) was placed. The cells were then allowed to migrate through to the lower chamber and adhere to the underside of the membrane for 4 h, at which point the cells were fixed with 70% (v/v) ethanol and 4′,6-diamidino-2-phenylindole (DAPI) stained. Cells on the upper surface of the polycarbonate membrane were removed with cotton swabs, while those that had migrated through the membrane and were bound to the lower surface of the membrane were enumerated by cell imaging and integrated morphometry analysis.

Cell proliferation, cytotoxicity, and apoptosis assays

For cell proliferation measurements, a standard colorimetric assay was performed according to the manufacturer's instructions (Cell Titer96; Promega). In brief, this assay quantified the presence of NADH or NADPH dehydrogenases that were produced by metabolically active cells. These activities were measured by the reduction of tetrazolium compounds to formazan products that could be quantified by spectrophotometry. WT and Irgm1-deficient BMM were plated at equal densities in 96-well plates and cultured for 24 h. They were then exposed to 100 U/ml IFN-γ or control conditions for an additional 24 h. After addition of the tetrazolium reagent to the culture wells and incubation at 37°C, absorbance at 490 nm was read on a standard plate reader to determine the relative levels of proliferation among the cell populations. Each condition was performed in triplicate.

For cellular cytotoxicity assays, a standard lactate dehydrogenase (LDH) release assay was performed according to the manufacturer's instructions (no. G1781; Promega). BMM were cultured under control conditions or in the presence of 100 U/ml IFN-γ for 24 h. Conditioned medium were then isolated from the cells and used for colorimetric determination at 490 nm of LDH that may have been released by necrotic cells. Each condition was performed in octuplicate. Parallel groups of cells were lysed by repeated freezing and thawing to determine the total LDH content of the cells.

For apoptosis, a standard annexin V-binding assay was used according to the manufacturer's instructions (no.V13241; Molecular Probes). BMM were cultured under control conditions or in the presence of 100 U/ml IFN-γ for 24 h. The cells were then harvested and used for the annexin V-Alexa Fluor-488/propidium iodide staining. The stained cells were analyzed by flow cytometry to determine the percentages that were annexin V positive (apoptotic) and/or propidium iodide positive (necrotic).

Cell staining

BMM were plated onto fibronectin-coated or uncoated glass coverslips, cultured ~24 h, and then cultured an additional 24 h in the presence of IFN-γ, as indicated. The cells were fixed with 4% paraformaldehyde (w/v) in PBS for 15 min and permeabilized with 0.2% (w/v) saponin in PBS for 10 min. The cells were then stained with 10 U/ml phalloidin-conjugated

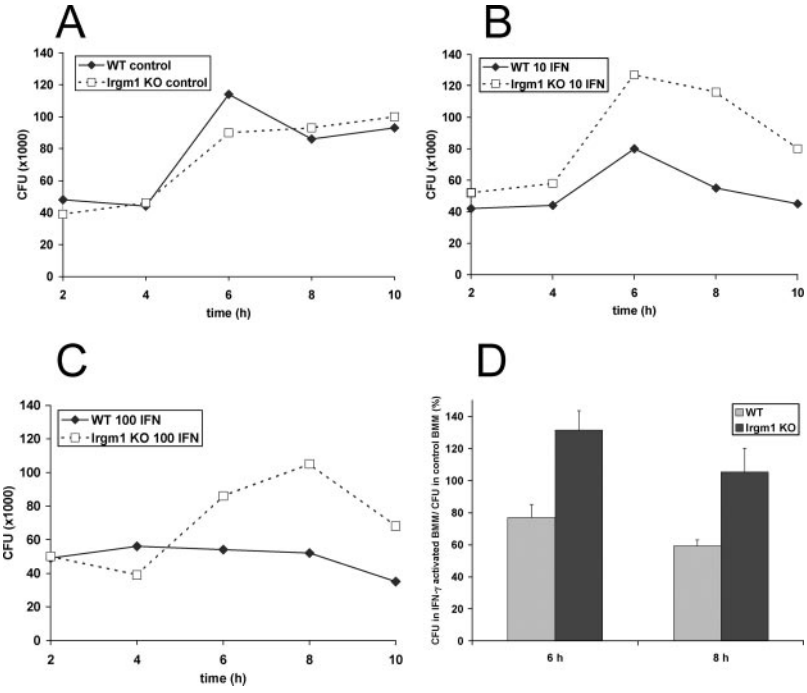

FIGURE 4. Impaired IFN-γ-induced suppression of *S. typhimurium* growth in Irgm1-deficient macrophages. *A–C*, WT and Irgm1 KO BMM were cultured for 24 h under control conditions (*A*) or in the presence of 10 or 100 U/ml IFN-γ (*B* and *C*, respectively). The cells were subsequently infected with *S. typhimurium* SL1344 at a multiplicity of infection of 2:1. After the indicated times in medium containing gentamicin to inhibit extracellular bacterial growth, CFUs were determined. Shown is a representative experiment. *D*, The average effect of IFN-γ on *S. typhimurium* persistence was calculated for seven experiments and expressed as a function of the number of CFU recovered from BMM activated with 100 U/ml IFN-γ, divided by the number of CFU recovered from BMM cultured under control conditions, at the indicated time points. Error bars, SEM. The decreased effect of IFN-γ activation in Irgm1 KO BMM was statistically significant at both 6 and 8 h ($p = 0.00032$ and $p = 0.0099$, respectively).

Downloaded from http://www.jimmunol.org/ by guest on July 19, 2018

Alexa Fluor 594 to stain actin (Molecular Probes) and with anti-phosphopaxillin-[pY^{118}] (BioSource International/Invitrogen Life Technologies) followed by Alexa Fluor 488-conjugated secondary Abs (Molecular Probes). Cell imaging and analysis were performed using an Olympus IX70 microscope linked to a computer outfitted with AutoQuant 9.3 (Media Cybernetics) and MetaMorph 6.2.3.5 (Molecular Devices Corporation) software.

Statistical Analysis

Student's paired *t test was used* to assess statistical significance where appropriate.

Results

Decreased resistance to S. typhimurium *in Irgm1 (LRG-47)-deficient mice*

We first tested whether Irgm1 (LGR-47)-deficient mice had decreased resistance to *S. typhimurium*, a bacterium that proceeds with an acute infection and has an essentially exclusive vacuolar lifestyle within a host cell. Previous work had focused on the role of Irgm1 in resistance to bacteria that chronically infect host cells and maintain a vacuolar lifestyle, *Mycobacterium avium* (34) and *M. tuberculosis* (24), or bacteria that infect acutely but maintain a predominantly cytosolic lifestyle, *L. monocytogenes* (18). To begin the current studies, we infected Irgm1-deficient mice that had been generated on a mixed C57BL/6-129SvImJ background and found that they had significantly reduced resistance to *S. typhimurium* compared with WT mice, as manifested by their decreased survival following infection (Fig. 1*A*) and increased bacterial loads in spleen and liver (Fig. 1*B*). Because resistance to *S. typhimurium* differs significantly between the C57BL/6 and 129SvImJ strains (in part as consequence of differential NRAMP-1 function (35, 36)), potentially confounding the data from C57BL/6-129SvImJ mice, we backcrossed Irgm1-deficient mice onto a pure C57BL/6 background and onto a pure 129SvImJ background and then tested the two groups of mice. On either background, Irgm1-deficient mice demonstrated significantly decreased resistance to the bacterium compared with WT mice (Fig. 1, *C* and *D*). Similar results were obtained in these studies when the bacteria were administered to the mice i.v. (Fig. 1) or intragastrically (data not shown). In contrast, Irgm3 (IGTP)- and Irgd (IRG-47)-deficient mice displayed normal resistance to *S. typhimurium* when either survival (Fig. 1*A*) or bacterial loads (data not shown) were assessed. Thus, Irgm1 is uniquely required among these three IRG proteins for resistance to *S. typhimurium*. For the remaining studies, we concentrated on Irgm1, using mice and cells derived from the mice on the C57BL/6 background only.

Impaired granuloma formation in Irgm1-deficient mice

We next examined the histology of livers and spleens from Irgm1-deficient mice from days 2 and 5 postinfection (Fig. 2). These time points were chosen based on the observations that Irgm1 expression in WT mice reached maximal levels at day 2 following infection, and high expression was maintained at least through day 5 (data not shown). At a gross level, the livers of both WT and Irgm1-deficient mice appeared slightly pale at day 2; but by day 5, the color of the WT liver had resolved to a normal tan/red color, while that of the Irgm1-deficient mouse had become even paler, perhaps indicating an unresolved inflammatory process. The weights of the spleens were monitored over the same time period and were found to increase in both types of mice, but at a slower rate in the Irgm1-deficient mice, so that by day 5 the splenic weights of Irgm1-deficient mice were ~60% of those of WT mice. Histologically, in both WT and Irgm1-deficient mice at 2 days postinfection, inflammatory foci were present in spleen (Fig. 2*A*) and liver (Fig. 2*B*) composed primarily of polymorphonuclear

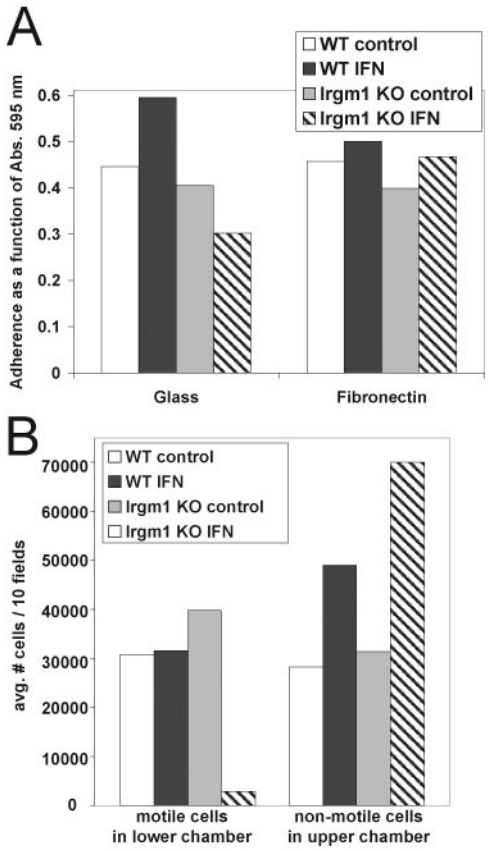

FIGURE 5. Decreased adhesion and motility of Irgm1-deficient macrophages. *A*, Adhesion: WT and Irgm1 KO BMM were cultured at equal densities on glass coverslips that were uncoated or coated with fibronectin as indicated. The cells were then exposed to 100 U/ml IFN-γ or control conditions for 24 h. Adherence was assessed by washing off loosely adherent cells, staining the remaining adherent cells with crystal violet, solubilizing them, and measuring absorbance of the lysate as an indicator of adherence. Shown is a representative experiment. The decrease in adherence to glass in IFN-γ-activated Irgm1 KO BMM was statistically significant over three experiments, for which the average ratio of adherence of IFN-γ-activated cells to adherence of control cells was 121.3 ± 5.8% (SEM) for WT BMM and 62.4 ± 8.7% for Irgm1 KO BMM ($p = 0.012$). *B*, Motility: WT and Irgm1-deficient BMM were maintained under control conditions or were activated with 100 U/ml IFN-γ for 24 h, and they were then placed in equal numbers in the upper chambers of Transwell apparatuses. The medium in lower chambers, but not upper chambers, contained M-CSF as a chemoattractant. Cells that migrated through the membrane and attached to the fibronectin-coated underside over a 4-h period were stained with DAPI, whereas those that remained in the upper chamber were removed by swabbing. As a control in the same experiment, cells in separate Transwells that remained on the upper surface of the membrane were stained with DAPI, whereas those that had migrated to the lower surface of the membrane were removed by swabbing. In both cases, the cells were imaged and quantified by measuring the total DAPI-positive area on the filter using software image analysis. Shown is a representative study. The decrease in motility of IFN-γ-activated Irgm1 KO BMM was statistically significant: Over four experiments, the average ratio of motility of IFN-γ-activated cells to motility of control cells was 117 ± 23% (SEM) for WT BMM and 21 ± 13% for Irgm1 KO BMM ($p = 0.040$).

cells (PMNs). In the WT mice, these foci matured over the succeeding days, so that by day 5, they were well-organized granulomas containing primarily epithelioid and multinucleated giant cells of macrophage origin. In contrast, in the Irgm1-deficient mice, the foci did not mature to the same extent, but maintained their high PMN content and exhibited a rudimentary

Downloaded from http://www.jimmunol.org/ by guest on July 19, 2018

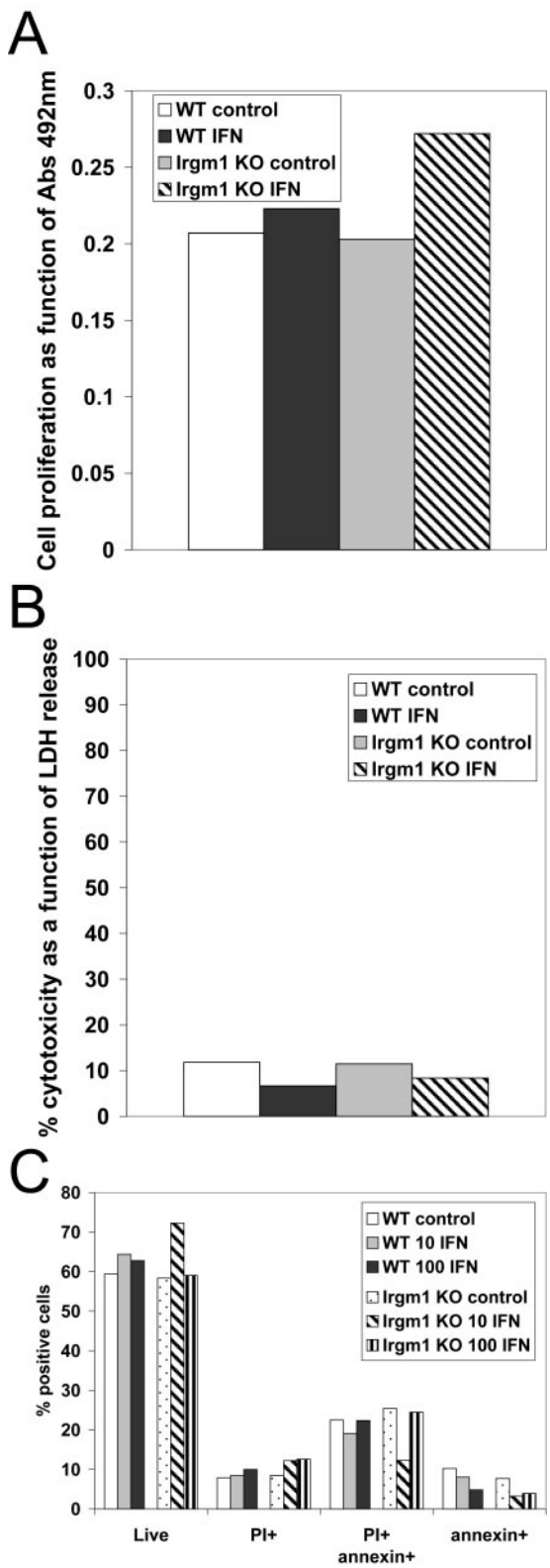

FIGURE 6. Normal cell proliferation, cytotoxicity, and apoptosis in IFN-γ-activated Irgm1-deficient macrophages. *A*, Cell proliferation: WT and Irgm1 KO BMM were plated at equal densities and cultured for 24 h. They were then exposed to 100 U/ml IFN-γ or to control conditions for an additional 24 h. Relative NADH and NADPH hydrogenase levels in culture supernatants were determined as a measure of cell proliferation. Shown are average measurements in a representative of three experiments. *B*, Cytotoxicity: WT and Irgm1 KO BMM were plated at equal densities and cultured for 24 h. They were then exposed to 100 U/ml IFN-γ or to control conditions for an additional 24 h. Conditioned supernatants were then isolated from the cells and used for a colorimetric LDH release assay as a measure of cytotoxicity. Detected levels of LDH are expressed as the percentage of the total LDH that was present when the cells were completely lysed. Shown are average measurements in a representative of three experiments. *C*, Apoptosis: WT C57BL/6 and Irgm1 KO BMM were cultured for 24 h under control conditions or in the presence of 10 or 100 U/ml IFN-γ. The cells were then labeled with annexin V to indicate apoptotic cells and/or propidium iodide (PI) to indicate advanced necrotic cells. Labeled cells were analyzed by FACS; 10,000 events were captured for each sample. Shown are percent positive cells in a representative of three experiments.

epithelioid cell response (Fig. 2, *A–C*). Thus, the ability of the Irgm1-deficient mice to mount a granulomatous response and to concentrate cells of macrophage origin at the sites of bacterial deposition was impaired.

The deficient granulomatous response in the liver and spleen of Irgm1-deficient mice implied that either macrophages were not present in these tissues or that they were present but not incorporated into well-defined granulomas. To address these possibilities, flow cytometry was used to examine the leukocyte composition of the spleens of WT and Irgm1-deficient mice at 5 days after *S. typhimurium* infection (Fig. 3). Using this approach, macrophage frequency did not increase in the spleens of Irgm1-deficient mice following infection, whereas it increased severalfold in the spleens of WT mice at 5 days following infection. In contrast, neutrophils and T cells displayed similar dynamics in WT and Irgm1-deficient mice, with neutrophils increasing markedly following infection and the T cells decreasing, both of which are typical responses to *S. typhimurium* (33). Thus taken together, the histological and FACS analyses suggested that there was an impairment in the macrophage compartment in Irgm1-deficient mice following *S. typhimurium* infection.

Several underlying mechanisms could lead to impaired macrophage responses in Irgm1-deficient mice, including the possibilities of decreased production of macrophages in the mice, decreased intracellular killing by macrophages leading to macrophage cytotoxicity, and impaired trafficking of macrophages to the granulomas/sites of infection. The first of these seemed unlikely, since macrophage pools in the spleen (Fig. 3) and peripheral blood (data not shown) were not decreased in Irgm1-deficient mice before infection. In the remaining studies described here, we focused on the other two possibilities by using in vitro assays to assess intracellular killing of *S. typhimurium* in Irgm1-deficient macrophages and to assess motility of Irgm1-deficient macrophages.

Decreased intracellular killing of S. typhimurium *in Irgm1-deficient macrophages*

It has been shown previously that Irgm1 mediates the ability of IFN-γ to restrict the growth of *M. tuberculosis* (24), *T. cruzi* (25), and *T. gondii* (22) in cultured macrophages. However, in studies involving *M. avium*, absence of Irgm1 did not have a significant effect on the ability of IFN-γ to restrict bacterial growth (34), suggesting that the ability of Irgm1 to affect bacterial survival in macrophages may not be a general function of the protein in all contexts. In this study, we tested whether Irgm1 mediated the ability of IFN-γ to restrict the growth of *S. typhimurium* using gentamicin protection assays. BMM were isolated and activated with different concentrations of IFN-γ before infecting them with *S. typhimurium* and examining bacterial survival. In WT cells, *S. typhimurium* showed a small growth phase that peaked after 6–8 h (Fig. 4*A*). This growth phase was suppressed when the WT BMM

Downloaded from http://www.jimmunol.org/ by guest on July 19, 2018

were activated with IFN-γ (Fig. 4, *B* and *C*). However, in Irgm1-deficient BMM, the effect of IFN-γ was mostly ablated when 10 U/ml IFN-γ was used to activate the cells, and it was also significantly muted at the higher dose of 100 U/ml IFN-γ (Fig. 4). The effect of Irgm1 deficiency was similar whether the virulent SL1344 strain (Fig. 4) or an aroA$^-$ strain (data not shown) was examined, although it was more pronounced using the virulent strain. Thus, the ability of Irgm1-deficient BMM to restrict the growth of *S. typhimurium* in response to IFN-γ activation was compromised. Nevertheless, it should be noted that in these assays, Irgm1-deficienct BMM retain some ability to restrict the growth of *S. typhimurium* and, furthermore, that the impact on controlling the growth of *S. typhimurium* in BMM following activation with IFN-γ was not as striking as the impact on controlling the growth of other pathogens such as *T. gondii*, where even at high doses of IFN-γ (100 U/ml), the cytokine induced little pathogen growth restriction in absence of Irgm1 (22). This prompted further investigation into the functioning of Irgm1-deficient macrophages.

Decreased adhesion and motility of Irgm1-deficient macrophages in vitro

One possibility raised by lack of Irgm1-deficient macrophages at sites of *S. typhimurium* deposition in vivo was that the ability of the macrophages to migrate to these sites was impaired. If migration of Irgm1-deficient macrophages was impaired in vivo, then it would likely be reflected in loss of adhesive and/or motile properties of Irgm1-deficient macrophages in vitro. Consequently, adhesion and motility of Irgm1-deficient BMM were tested using in vitro assays (Fig. 5). Adhesion of WT and Irgm1-deficient BMM to glass coverslips was comparable under basal cell growth conditions (Fig. 5*A*). However, after activation of the cells with IFN-γ, there was a marked loss of adherence in Irgm1-deficient BMM, whereas in WT BMM there was an increase in adhesion. When the same experiments were performed on coverslips that had been coated with fibronectin, adherence of the LRG-47 knockout (KO) BMM was restored (Fig. 5*A*), as it was when the cells were cultured on tissue culture-treated plastic dishes (data not shown).

The motile properties of Irgm1-deficient BMM were next assessed using standard Transwell assays, which measured the ability of cells to move from an upper chamber through small pores in a membrane into the lower chamber and then bind to the underside of the membrane (Fig. 5*B*). WT and Irgm1-deficient BMM were found to migrate with about the same efficiency when the cells were cultured under basal growth conditions. However, after the cells were activated with IFN-γ, Irgm1-deficient BMM displayed a marked decrease in the number of the cells that passed through the membrane and bound to its underside, indicating that their motility was greatly impaired (Fig. 5*B*). Quantification of the cells remaining in the upper chamber following the incubation indicated that the Irgm1-deficient macrophages did indeed remain in the upper chamber (Fig. 5*B*). Additionally, to ensure that some cells were not traveling through the membrane but failing to adhere to it and falling to the bottom of the chamber, cells at the bottom of the lower chambers were enumerated; however, very few IFN-γ-activated Irgm1-deficient BMM were present in the bottom of the lower chambers (data not shown). Together, these results suggest that Irgm1 is required to maintain normal motility of IFN-γ-activated macrophages.

Normal levels of cell proliferation, cytotoxicity, and apoptosis in cultured Irgm1-deficient macrophages

Several standard approaches were used to determine whether the loss of adherence and motility of activated Irgm1-deficient BMM could have resulted secondarily as a consequence of enhanced cytotoxicity or apoptosis in those cells. Cell proliferation was measured using a standard assay in which NADH and NADPH dehydrogenase production by replicating cells was quantified (Fig. 6*A*); cellular cytotoxicity was measured by LDH release from dying cells (Fig. 6*B*); and apoptosis was measured by annexin V staining (Fig. 6*C*). By these approaches, IFN-γ-activated Irgm1-deficient

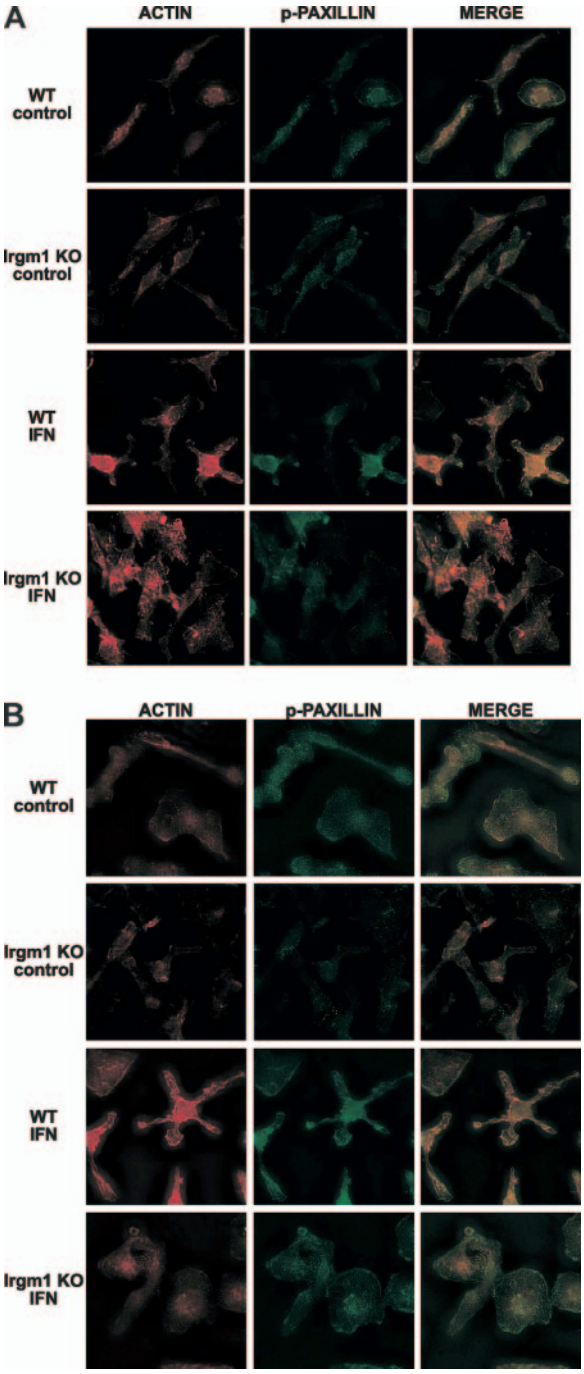

FIGURE 7. Altered morphology and cellular adhesions in IFN-γ-activated macrophages lacking Irgm1. WT and Irgm1-deficient BMM were plated at equal densities on uncoated (*A*) or fibronectin-coated (*B*) coverslips. The cells were exposed to control conditions or to 100 U/ml IFN-γ for 24 h. They were then fixed and stained with phalloidin (red) or anti-[Y^{118}]-paxillin (green). Colocalization of actin and [Y^{118}]-paxillin indicate areas of adhesion to the substratum. Note that the same cells are enumerated in Table I.

Downloaded from http://www.jimmunol.org/ by guest on July 19, 2018

Table I. *Enumeration of macrophage phenotypes in WT and Irgm1-deficient BMM*

Cells	Substrate	Treatment	No. of Cells (per 5 fields)	% Nonpolar/ rounded	% Polar/Well-Formed Lamellipodia
WT	Glass	Control	979	5	95
Irgm1 KO	Glass	Control	792	3	97
WT	Glass	100 U/ml IFN-γ	1155	4	96
Irgm1 KO	Glass	100 U/ml IFN-γ	502	6	94
WT	Fibronectin	Control	1354	23	77
Irgm1 KO	Fibronectin	Control	1788	18	82
WT	Fibronectin	100 U/ml IFN-γ	1386	21	79
Irgm1 KO	Fibronectin	100 U/ml IFN-γ	1141	63	37

BMM were found to replicate at comparable rates to those of activated WT BMM, to manifest low levels of cytotoxicity that were statistically the same as those of activated WT cells, and to display low levels of apoptosis that were again statistically the same as those of activated WT cells (Fig. 6 and data not shown). In addition, apoptosis was assessed by a microscopic assay to examine nuclear condensation, and, again, the frequency of apoptotic cells among activated Irgm1-deficient BMM was found to be very low (<1% of cells) and comparable to the frequency found in activated WT BMM (data not shown). Thus, by these measures, Irgm1-deficient BMM did not display increased levels of cytotoxicity or apoptosis.

Altered morphology of Irgm1-deficient macrophages

Irgm1-deficient cells were observed microscopically to assess their overall morphology, adhesion-associated proteins, and actin cytoskeleton (Fig. 7 and Table I). These parameters were examined on both uncoated glass and fibronectin-coated substrates. On both glass and fibronectin under control conditions, WT and Irgm1 cells displayed a similar distribution of morphologies that ranged from nonpolar cells that were round and flattened to polar cells with well-formed lamellopoidia (Table I). In addition, under control growth conditions, actin staining and the level and distribution of actin/[pY^{118}]-paxillin-positive foci appeared similar (Fig. 7). Note that it has been established previously that macrophage adhesions/podosomes can be identified by phalloidin and anti-[pY^{118}]-paxillin costaining (37).

When the cells were activated with IFN-γ, there were marked differences between Irgm1-deficient and WT BMM on both substrates (Fig. 7). When cultured on glass, activated Irgm1-deficient BMM tended to forms clumps and detach, while activated WT cells did not (Fig. 7*A*). However, the ratio of nonpolar:polar morphologies in the activated Irgm1-deficient cells that remained on the glass substrate was similar to that in activated WT cells (Table I). Also on glass, activated Irgm1-deficient cells displayed a striking decrease in actin/[Y^{118}]-paxillin-positive foci, which was in keeping with their decreased adhesion to glass (Fig. 5*A* and Table I). Additionally, the actin cytoskeleton appeared to be disorganized in activated Irgm1-deficient cells and did not manifest the evenly distributed punctate pattern of activated WT BMM (Fig. 7*A*).

When cultured on fibronectin-coated glass (Fig. 7*B*), the morphology of activated Irgm1-deficient BMM was markedly different from their morphology on uncoated glass. On fibronectin, there was a higher degree of large, round, and flattened cells relative to polar cells with well-formed lamellipodia (Table I), suggesting fewer motile cells among the activated Irgm1-deficient population. (Macrophages with a large, round morphology have been demonstrated previously to be nonmotile (38).) The activated Irgm1-deficient cells showed a higher degree of actin/[Y^{118}]-paxillin-positive foci on fibronectin than they did on uncoated glass at levels comparable to the amounts seen in activated WT cells on both substrates, which was in keeping with the observed strong adhesion of activated Irgm1-deficient cells to fibronectin but not glass (Fig. 5*A*). In addition, the activated Irgm1-deficient cells displayed much weaker actin staining than did activated WT BMM.

In summary, there were striking differences in the morphology, adhesion-associated proteins, and actin staining of IFN-γ-activated Irgm1-deficient BMM, as compared with activated WT cells. These changes were consistent with the losses in adhesion and motility displayed by Irgm1-deficient macrophages and support the overall finding that Irgm1 is a critical factor that regulates these processes.

Discussion

In the current work, we demonstrate that Irgm1 (LRG-47) deficiency leads to decreased resistance to *S. typhimurium* in mice, characterized by decreased survival, increased bacterial loads, and a failure to concentrate macrophages at sites of bacterial deposition in the spleen and liver. Underscoring this phenotype was a marked decrease in basic macrophage functions, including intracellular bacterial killing and adhesion/motility. Thus, these results corroborate what has been demonstrated previously for other pathogens, that Irgm1 is a key factor required for resistance to intracellular bacteria and protozoa. However, they further suggest that Irgm1 has much broader functions in regulating the activated macrophage, particularly in controlling its adhesion and movement. Regulation of the motility of activated macrophages is likely to be a key mechanism through which Irgm1 controls resistance to pathogens such as *S. typhimurium*.

Our previous work and that of others have suggested that Irgm1, as well as other IRG proteins, function in part by localizing to pathogen-containing vacuoles in macrophages and other host cells, where they control the processing of those vacuoles and promote eradication of the pathogens (9). The current results raise the question of how Irgm1 might play roles in both vacuole processing and its newly ascribed function, the regulation of motility and adhesion of activated macrophages. One answer is suggested by comparison of Irgm1 with a group of related proteins, the dynamins. These GTPases were originally characterized as proteins that control vesicle budding at the plasma membrane and in the Golgi (for review, see Ref. 39). Like the IRG proteins, the dynamins are able to form short polymers, and it is contraction of dynamin polymers in association with cellular membranes and the actin cytoskeleton that leads to deformation of the membrane and the "pinching off" of vesicles. Recent work suggests dynamin function goes well beyond the process of endocytosis; in fact, dynamins also play an intimate role in cell adhesion and migration. Dynamins are thought to accomplish this by direct interaction with structures that are important for cell motility and adhesion, including focal adhesions, podosomes, and lamellipodia, as well as by interacting with the actin cytoskeleton. Hence, dynamin shares several properties with Irgm1 including localization to the Golgi and plasma membrane

Downloaded from http://www.jimmunol.org/ by guest on July 19, 2018

(20, 22), the ability to multimerize (40), involvement in vacuole processing (20–22, 24, 27), modulation of cell motility (current work), and regulation of actin remodeling (current work).

Future studies should focus on the molecular mechanism through which Irgm1 regulates adhesion and motility in activated macrophages. As with the dynamins, this may well occur by modulating cytoskeletal remodeling, which could be a central function of Irgm1 as it would impact many processes including cell motility, vacuolar processing/trafficking, and authophagy. In the current work, absence of Irgm1 led to altered actin staining in macrophages. Another IRG protein, Irga6, has also been linked to the cytoskeleton. In yeast two-hybrid studies, it was found to be a binding partner for the microtubule binding protein hook3 (41), although the significance of this finding for host resistance and general cellular physiology is unknown. A second possible mechanism through which Irgm1 may influence macrophage adhesion and motility is the regulation of endocytic recycling pathways that modulate expression of adhesion receptors on the cell surface. Although there is currently no specific evidence to support this possibility, the general involvement of Irgm1 in vacuolar dynamics suggests that it may also regulate endocytic vacuole trafficking. Certainly, there are many well-known GTPase families that regulate vacuole trafficking, such as the rab proteins. There is also a growing body of literature that demonstrates a connection between cell adhesion/motility and endocytic recycling (42).

In the current work, we show deficiencies in that ability of *S. typhimurium* granulomas to mature to epithelioid cell-rich lesions in Irgm1-deficient mice. Altered characteristics of Irgm1-deficient granulomas have also been noted following *M. avium* infection. However, in that setting, a change in the macrophage content was not noted, rather the granulomas were found to be less compact and lacking a characteristic cuff of lymphocytes around their perimeters (34). In the case of the *S. typhimurium* granulomas, there are several likely possibilities that would lead to absence of macrophages in the granulomas. Based on the data described here, one possibility is that, because Irgm1-deficient macrophages have altered adhesive and motile properties, they are impaired in their ability to migrate to sites of *S. typhimurium* deposition. An additional possibility is that decreased intracellular killing of *S. typhimurium* in macrophages could lead to bacteria-induced cytotoxicity that would deplete granulomas of macrophages. Other possibilities that we cannot formally exclude are that production of chemokines that attract macrophages to granulomas is suppressed in Irgm1-deficient mice or that apoptosis is enhanced in Irgm1-deficient macrophages. Addressing the latter, we found that levels of apoptosis are not increased in Irgm1-deficient macrophages in vitro, though this does not necessarily indicate that apoptosis may not be increased in vivo in the setting of *S. typhimurium* infection. Future studies should address further the mechanism that leads to impaired maturation of *S. typhimurium* granulomas.

In conclusion, our studies indicate that Irgm1 is a key protein that is produced in response to IFN-γ, because it enables critical aspects of the activated macrophage phenotype. These include enhanced intracellular killing capacities and altered adhesive and motile properties that may allow the cells to traffic to sites of pathogens more efficiently. The molecular basis for these functions, and the roles of other IRG proteins in these processes, will be addressed in future studies.

Acknowledgments

We are grateful to Herman Staats for assistance with the *S. typhimurium* studies. We are also grateful to Brice Weinberg and the Duke University Bacterial Pathogenesis group for helpful discussions.

Disclosures

The authors have no financial conflict of interest.

References

1. Boehm, U., T. Klamp, M. Groot, and J. C. Howard. 1997. Cellular responses to interferon-γ. *Annu. Rev. Immunol.* 15: 749–795.
2. Stark, G. R., I. M. Kerr, B. R. Williams, R. H. Silverman, and R. D. Schreiber. 1998. How cells respond to interferons. *Annu. Rev. Biochem.* 67: 227–264.
3. Ehrt, S., D. Schnappinger, S. Bekiranov, J. Drenkow, S. Shi, T. R. Gingeras, T. Gaasterland, G. Schoolnik, and C. Nathan. 2001. Reprogramming of the macrophage transcriptome in response to interferon-γ and *Mycobacterium tuberculosis*: signaling roles of nitric oxide synthase-2 and phagocyte oxidase. *J. Exp. Med.* 194: 1123–1140.
4. Schroder, K., P. J. Hertzog, T. Ravasi, and D. A. Hume. 2004. Interferon-γ: an overview of signals, mechanisms and functions. *J. Leukocyte Biol.* 75: 163–189.
5. MacMicking, J. D. 2004. IFN-inducible GTPases and immunity to intracellular pathogens. *Trends Immunol.* 25: 601–609.
6. Taylor, G. A., C. G. Feng, and A. Sher. 2004. p47 GTPases: regulators of immunity to intracellular pathogens. *Nat. Rev. Immunol.* 4: 100–109.
7. Bekpen, C., J. P. Hunn, C. Rohde, I. Parvanova, L. Guethlein, D. M. Dunn, E. Glowalla, M. Leptin, and J. C. Howard. 2005. The interferon-inducible p47 (IRG) GTPases in vertebrates: loss of the cell autonomous resistance mechanism in the human lineage. *Genome Biol.* 6: R92.
8. MacMicking, J. D. 2005. Immune control of phagosomal bacteria by p47 GTPases. *Curr. Opin. Microbiol.* 8: 74–82.
9. Taylor, G. A. 2007. IRG proteins: key mediators of interferon-regulated host resistance to intracellular pathogens. *Cell. Microbiol.* 9: 1099–1107.
10. Sorace, J. M., R. J. Johnson, D. L. Howard, and B. E. Drysdale. 1995. Identification of an endotoxin and IFN-inducible cDNA: possible identification of a novel protein family. *J. Leukocyte Biol.* 58: 477–484.
11. Boehm, U., L. Guethlein, T. Klamp, K. Ozbek, A. Schaub, A. Futterer, K. Pfeffer, and J. C. Howard. 1998. Two families of GTPases dominate the complex cellular response to IFN-γ. *J. Immunol.* 161: 6715–6723.
12. Taylor, G. A., M. Jeffers, D. A. Largaespada, N. A. Jenkins, N. G. Copeland, and G. F. Woude. 1996. Identification of a novel GTPase, the inducibly expressed GTPase, that accumulates in response to interferon γ. *J. Biol. Chem.* 271: 20399–20405.
13. Gilly, M., and R. Wall. 1992. The IRG-47 gene is IFN-γ induced in B cells and encodes a protein with GTP-binding motifs. *J. Immunol.* 148: 3275–3281.
14. Carlow, D. A., J. Marth, I. Clark-Lewis, and H. S. Teh. 1995. Isolation of a gene encoding a developmentally regulated T cell-specific protein with a guanine nucleotide triphosphate-binding motif. *J. Immunol.* 154: 1724–1734.
15. Lafuse, W. P., D. Brown, L. Castle, and B. S. Zwilling. 1995. Cloning and characterization of a novel cDNA that is IFN-γ-induced in mouse peritoneal macrophages and encodes a putative GTP-binding protein. *J. Leukocyte Biol.* 57: 477–483.
16. Bernstein-Hanley, I., J. Coers, Z. R. Balsara, G. A. Taylor, M. N. Starnbach, and W. F. Dietrich. 2006. The p47 GTPases Igtp and Irgb10 map to the *Chlamydia trachomatis* susceptibility locus Ctrq-3 and mediate cellular resistance in mice. *Proc. Natl. Acad. Sci. USA* 103: 14092–14097.
17. Taylor, G. A., C. M. Collazo, G. S. Yap, K. Nguyen, T. A. Gregorio, L. S. Taylor, B. Eagleson, L. Secrest, E. A. Southon, S. W. Reid, et al. 2000. Pathogen-specific loss of host resistance in mice lacking the IFN-γ-inducible gene IGTP. *Proc. Natl. Acad. Sci. USA* 97: 751–755.
18. Collazo, C. M., G. S. Yap, G. D. Sempowski, K. C. Lusby, L. Tessarollo, G. F. Woude, A. Sher, and G. A. Taylor. 2001. Inactivation of LRG-47 and IRG-47 reveals a family of interferon γ-inducible genes with essential, pathogen-specific roles in resistance to infection. *J. Exp. Med.* 194: 181–188.
19. Taylor, G. A., R. Stauber, S. Rulong, E. Hudson, V. Pei, G. N. Pavlakis, J. H. Resau, and G. F. Vande Woude. 1997. The inducibly expressed GTPase localizes to the endoplasmic reticulum, independently of GTP binding. *J. Biol. Chem.* 272: 10639–10645.
20. Martens, S., K. Sabel, R. Lange, R. Uthaiah, E. Wolf, and J. C. Howard. 2004. Mechanisms regulating the positioning of mouse p47 resistance GTPases LRG-47 and IIGP1 on cellular membranes: retargeting to plasma membrane induced by phagocytosis. *J. Immunol.* 173: 2594–2606.
21. Martens, S., I. Parvanova, J. Zerrahn, G. Griffiths, G. Schell, G. Reichmann, and J. C. Howard. 2005. Disruption of *Toxoplasma gondii* parasitophorous vacuoles by the mouse p47-resistance GTPases. *PLoS Pathog.* 1: e24.
22. Butcher, B. A., R. I. Greene, S. C. Henry, K. L. Annecharico, J. B. Weinberg, E. Y. Denkers, A. Sher, and G. A. Taylor. 2005. p47 GTPases regulate *Toxoplasma gondii* survival in activated macrophages. *Infect. Immun.* 73: 3278–3286.
23. Halonen, S. K., G. A. Taylor, and L. M. Weiss. 2001. Gamma interferon-induced inhibition of *Toxoplasma gondii* in astrocytes is mediated by IGTP. *Infect. Immun.* 69: 5573–5576.
24. MacMicking, J. D., G. A. Taylor, and J. D. McKinney. 2003. Immune control of tuberculosis by IFN-γ-inducible LRG-47. *Science* 302: 654–659.
25. Santiago, H. C., C. G. Feng, A. Bafica, E. Roffe, R. M. Arantes, A. Cheever, G. Taylor, L. Q. Vierira, J. Aliberti, R. T. Gazzinelli, and A. Sher. 2005. Mice deficient in LRG-47 display enhanced susceptibility to *Trypanosoma cruzi* infection associated with defective hemopoiesis and intracellular control of parasite growth. *J. Immunol.* 175: 8165–8172.
26. Koga, R., S. Hamano, H. Kuwata, K. Atarashi, M. Ogawa, H. Hisaeda, M. Yamamoto, S. Akira, K. Himeno, M. Matsumoto, and K. Takeda. 2006. TLR-dependent induction of IFN-β mediates host defense against *Trypanosoma cruzi*. *J. Immunol.* 177: 7059–7066.

Downloaded from http://www.jimmunol.org/ by guest on July 19, 2018

27. Ling, Y. M., M. H. Shaw, C. Ayala, I. Coppens, G. A. Taylor, D. J. Ferguson, and G. S. Yap. 2006. Vacuolar and plasma membrane stripping and autophagic elimination of *Toxoplasma gondii* in primed effector macrophages. *J. Exp. Med.* 203: 2063–2071.
28. Gutierrez, M. G., S. S. Master, S. B. Singh, G. A. Taylor, M. I. Colombo, and V. Deretic. 2004. Autophagy is a defense mechanism inhibiting BCG and *Mycobacterium tuberculosis* survival in infected macrophages. *Cell* 119: 753–766.
29. Singh, S. B., A. S. Davis, G. A. Taylor, and V. Deretic. 2006. Human IRGM induces autophagy to eliminate intracellular mycobacteria. *Science* 313: 1438–1441.
30. Wray, C., and W. J. Sojka. 1978. Experimental *Salmonella typhimurium* infection in calves. *Res. Vet. Sci.* 25: 139–143.
31. Hoiseth, S. K., and B. A. Stocker. 1981. Aromatic-dependent *Salmonella typhimurium* are non-virulent and effective as live vaccines. *Nature* 291: 238–239.
32. VanCott, J. L., S. N. Chatfield, M. Roberts, D. M. Hone, E. L. Hohmann, D. W. Pascual, M. Yamamoto, H. Kiyono, and J. R. McGhee. 1998. Regulation of host immune responses by modification of *Salmonella* virulence genes. *Nat. Med.* 4: 1247–1252.
33. Kirby, A. C., U. Yrlid, and M. J. Wick. 2002. The innate immune response differs in primary and secondary *Salmonella* infection. *J. Immunol.* 169: 4450–4459.
34. Feng, C. G., C. M. Collazo-Custodio, M. Eckhaus, S. Hieny, Y. Belkaid, K. Elkins, D. Jankovic, G. A. Taylor, and A. Sher. 2004. Mice deficient in LRG-47 display increased susceptibility to mycobacterial infection associated with the induction of lymphopenia. *J. Immunol.* 172: 1163–1168.
35. Govoni, G., S. Vidal, S. Gauthier, E. Skamene, D. Malo, and P. Gros. 1996. The Bcg/Ity/Lsh locus: genetic transfer of resistance to infections in C57BL/6J mice transgenic for the Nramp1 Gly169 allele. *Infect. Immun.* 64: 2923–2929.
36. Govoni, G., and P. Gros. 1998. Macrophage NRAMP1 and its role in resistance to microbial infections. *Inflamm. Res.* 47: 277–284.
37. Wheeler, A. P., S. D. Smith, and A. J. Ridley. 2006. CSF-1 and PI 3-kinase regulate podosome distribution and assembly in macrophages. *Cell Motil. Cytoskeleton* 63: 132–140.
38. Neumeister, P., F. J. Pixley, Y. Xiong, H. Xie, K. Wu, A. Ashton, M. Cammer, A. Chan, M. Symons, E. R. Stanley, and R. G. Pestell. 2003. Cyclin D1 governs adhesion and motility of macrophages. *Mol. Biol. Cell* 14: 2005–2015.
39. Kruchten, A. E., and M. A. McNiven. 2006. Dynamin as a mover and pincher during cell migration and invasion. *J. Cell. Sci.* 119: 1683–1690.
40. Uthaiah, R. C., G. J. Praefcke, J. C. Howard, and C. Herrmann. 2003. IIGP1, an interferon-γ-inducible 47-kDa GTPase of the mouse, showing cooperative enzymatic activity and GTP-dependent multimerization. *J. Biol. Chem.* 278: 29336–29343.
41. Kaiser, F., S. H. Kaufmann, and J. Zerrahn. 2004. IIGP, a member of the IFN inducible and microbial defense mediating 47 kDa GTPase family, interacts with the microtubule binding protein hook3. *J. Cell. Sci.* 117: 1747–1756.
42. Jones, M. C., P. T. Caswell, and J. C. Norman. 2006. Endocytic recycling pathways: emerging regulators of cell migration. *Curr. Opin. Cell Biol.* 18: 549–557.

Downloaded from http://www.jimmunol.org/ by guest on July 19, 2018